

Advance in the Analysis Models for Characterizing Multi-Layered Interdigital Capacitors

Kwong Wai Mak* and Jianhua Hao

Department of Applied Physics, The Hong Kong Polytechnic University, Hong Kong, People's Republic of China

Abstract: The performances of multi-layered interdigital capacitors are commonly simulated by computer software. However, it is the time-consuming process. Besides simulations, the analytic models with closed form expressions provide convenient methods in particular usages, such as characterizing ferroelectric materials. This article briefly reviews the development in the expressions for analytic models. We provide an overview of partial capacitance technique and conformal mapping technique, which are used for formulating expressions. In addition, three common models used these techniques are presented. The differences of models and applications are also discussed.

Keywords: Device modeling, Interdigital capacitors, Conformal mapping, Ferroelectric devices.

INTRODUCTION

The performance of inter digital capacitors (IDCs) can be simulated by computer software. The software analyzes the complex structures using different method. For example, ANSYS's high frequency structure simulator (HFSS) uses 3D finite element method, Sonnet software uses fast Fourier transform-based analysis, and Agilent's Momentum uses method of moments.

A critical issue of computer simulation for IDCs is time-consuming. The first step of simulation is to slice the structure of IDCs into pieces. Then various methods are applied to each piece. The number of pieces determines the major part of computational time. Smaller the pieces are sliced, obviously more time and computational power is required, and accuracy is higher. However, the increment of accuracy by increasing piece number is limited while the piece size reduced to a certain value. In the case of IDCs involving extremely thin ferroelectric films (e.g., down to 0.1 micrometer) and commercially available substrates (e.g., several hundred micrometers), to get 5% accuracy using HFSS, several hours are required on nowadays workstations.

Besides simulation, analyzing the structure of IDCs has another approach. The aim of this approach is to create a suitable model to describe performance information using the basic parameters of IDCs. Models created are often presented in the closed form expressions. The accuracy is determined by the model itself.

Various models for IDCs have been suggested individually. These models use common techniques to resolve two major issues in analyzing IDCs. Firstly, the electric field distribution caused by interdigital electrodes (IDEs), the core component of IDCs, is non-uniform. Secondly, the boundary condition between substrates of IDCs may be changed because of the properties of substrates.

In this article, for further development of forming analytic models, the procedures and techniques used will be reviewed by analyzing the structure of IDE and substrates. The different between these models will be also discussed afterwards.

1. IDE STRUCTURE

The IDE structure is the starting point of analyzing IDCs. It is because the effective capacitance of IDCs is formed between in-plane electrode fingers of IDEs when the external voltage is applied across IDEs.

The basic structure of IDEs is comb-like as shown in Figure 1. To describe the structure, geometrical parameters are used. These parameters include finger

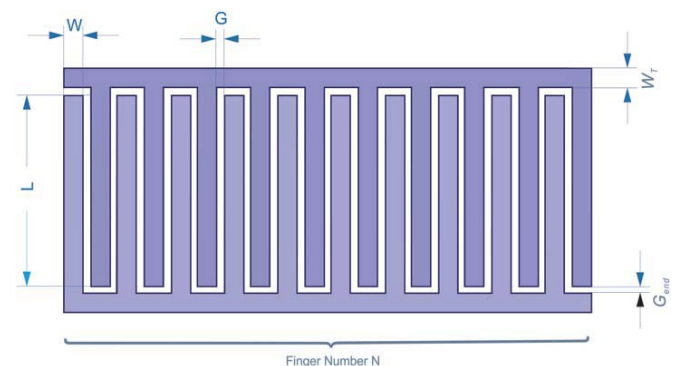


Figure 1: Scheme of interdigital electrodes.

*Address correspondence to this author at the Department of Applied Physics, The Hong Kong Polytechnic University, Hong Kong, People's Republic of China, Tel: +852 27664098; Fax: +852 23337629; E-mail: 11902340r@connect.polyu.hk

number N , finger width W , overlapping finger length L and the separation between each finger G . Also, additional parameters are used in some models, such as electrode thickness T , terminal width W_T and gaps at the end of the fingers G_{end} .

1.1. IDE Properties

If geometrical parameters reach the same scale of IDE thickness, the thickness effect should be accounted by using Wheeler's first order approximation[1]. The effective finger width W is:

$$W = W_{phy} + \left(\frac{T}{\pi}\right) \left[1 + \ln\left(\frac{4\pi W}{T}\right)\right] \tag{1}$$

where W_{phy} is the physical (geometric) width of electrode fingers. This case is common in IC technology, as parameters are in submicron scale. For example, electrode thickness is $0.1\mu\text{m}$ and the separation is between 2 to $5\mu\text{m}$, the different of physical and separation is about 5% to 10% due to this thickness effect. Thus it should be considered in analytic models when using the geometrical parameters of IDEs.

Furthermore, when electronic signal passes through IDCs, Rautio [2] suggests that for film thickness less than three times its skin depth, the equivalent line resistances due to the losses in metal strips may be approximated by:

$$r = \frac{1}{W\sigma_m\delta_s \left(1 - e^{-\frac{T}{\delta_s}}\right)} \tag{2}$$

where $\sigma_m(\text{S/m})$ is conductivity of the electrode metal, and δ_s is skin depth of metal.

$$\delta_s = \frac{1}{\sqrt{\pi\mu_o\sigma_m f}} \tag{3}$$

where μ_o is the magnetic constant of vacuum, and f is the operation frequency.

1.2. Conformal Mapping

The difficulty of analyzing the structure of IDCs is that the electric field in IDE is not straightly distributed between electrodes fingers like parallel capacitors.

Fortunately in most cases, there is no additional free charge in IDEs, the electrical potential outside the IDE satisfies Laplace's equation. A mathematical approach called conformal mapping (CM) becomes powerful tools to analyze the electrical potential distribution of whole IDCs.

The conformal mapping transforms a well-chosen region of IDCs, bounded by equipotential and continuous flux lines, into an equivalence of a parallel plate capacitor with the same electrical potential in a new coordinate system. To describe the conformal mapping independently in different models in the following sections, the analysis is simplified into the case that voltage U is applied to a pair of two adjacent fingers in IDEs with length L on a single layer substrate with thickness h . Figure 2(a) shows the cross-section; and (b) shows the final result of the transformation after applying CM technique.

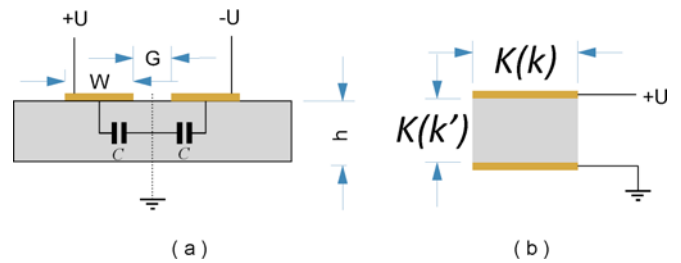


Figure 2(a): Scheme for a pair of two adjacent fingers in IDEs, **(b)** The result of final transformation.

Because of the symmetry of electric field in the layer generated by applied voltage, the middle plane can be treated as a magnetic wall, *i.e.* virtual ground. Thus the half side is analog to a parallel plate capacitor after the final step, which is the Schwarz-Christoffel transformation. The ratio of "parallel plate width" to "thickness" would be the ratio of the complete elliptic integral of first kind, with different modulus k and complementary modulus k' . The modulus k would be the function of W , G and interface position h relative to the electrode plane.

$$C(h) = \epsilon_o\epsilon_{eff} L \frac{K(k)}{K(k')} \tag{4}$$

In this expression, ϵ_{eff} is effective permittivity of the layer. $k' = \sqrt{1 - k^2}$ and $K(k)$ is the elliptic integrals of the first kind for the modulus k . The models use different CM steps, so there are different modulik in the Eq.(4).

2. MULTI-LAYERED STRUCTURE

The analysis of IDEs may lead to forming models for IDCs with a single substrate. However, it is still not able to analyze IDCs with multiple substrates or with materials covering IDEs. The common structure of these IDCs is a multi-layered structure. All substrates or materials covering IDEs are treated as layers.

A multi-layered structure of IDCs can be divided into two half-planes by IDEs, since the total effective properties can be equivalent to a single device formed by two half-plane devices connected in parallel.

The case will be discussed in this section similar to previous analysis of IDEs for simplifying discussion, but the IDCs with multiple substrates are used here. Figure 3 shows a cross-section of two adjacent fingers of IDEs in a three-layered structure IDC. The parameters of layers in analytic models include the interface position h , and the permittivity ϵ .



Figure 3: The cross-section of two adjacent fingers in IDEs with three-layered structure.

In capacitance calculation, the final capacitance is the sum of contributions from both half-planes. The half-plane capacitance is the superposition of each layer in the half-plane. It reflects the fact that electric field of positive electrodes of IDEs passes through each layer to reach the negative ones. However, the boundary of each layer causes different methods when one superposing the effect of each layers, due to their permittivity difference. Then according the method of superposition, various techniques are used and will be discussed.

2.1. Parallel Partial Capacitance Technique

In general use of ferroelectric material on commercially available substrate, the permittivity monotonic decreases from inner layer to outer layer away from the electrodes plane. Since the permittivity of inner layer is higher, the electric field is more concentrated in inner layer, but not all the electric field passes through the inner layer. The effective permittivity of inner layer would be smaller than the value of its native property. The effective value is the

result of the native property value subtracts the value of outer adjacent layer. Therefore, this technique is called parallel partial capacitance (PPC) technique as shown in Figure 4.

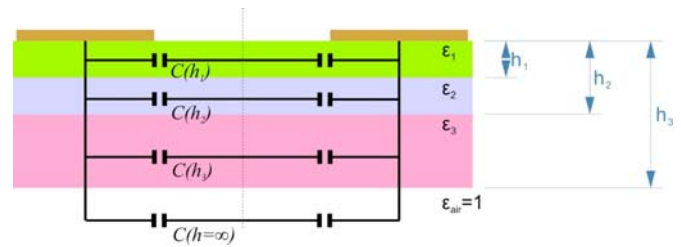


Figure 4: The scheme of parallel partial capacitance for three layer IDCs.

This technique was first proposed by Kochanov[3] for the study of transmission lines on dielectric exposing in air. The contribution of capacitances due to the dielectric is assumed that it has a relative permittivity $\epsilon_r - 1$. It indicates that the interface between the dielectric layer and the air layer between dielectric and air satisfies a Neumann boundary (NB) condition.

The NB condition for electric field is $\frac{\partial \phi}{\partial n} = \nabla \phi \cdot \hat{n} = 0$,

where ϕ is the electric potential and \hat{n} is a normal vector to the boundary. It was also applied by Veyres *et al.*[4] to express the capacitance of coplanar waveguides as a weighted sum of the capacitances of several layers. Then, Gevorgian *et al.* [5, 6] and Igreja and Dias[7, 8] both use this technique to obtain models for multi-layered structure IDCs.

2.2. Series Partial Capacitance Technique

There are a few cases that the permittivity monotonic increases from inner layer to outer layer away from the electrodes plane. Kitsara *et al.*[9] reported that case happened in an sensor of IDC with SiO₂/Si structure. Since the permittivity of outer layer is higher, the electric field is more concentrated in the outer layer, and penetrates though the interface between inner and outer layers. In this case, the electric field near the interface between two adjacent dielectric layers tends to be normal to the interfaces. Instead of NB condition, it is considered as a Dirichlet boundary (DB) condition. The DB condition for electric field is that the electric potential is a constant value along the boundary.

Ghione *et al.* [10] proposed series partial capacitance (SPC) technique for co-planar wave guide while Igreja and Dias[7] applied it to modeling the IDCs in this case. Compare to PPC technique, the effective permittivity of inner layer is the reciprocal result of the

reciprocal native property value subtracts the reciprocal value of outer adjacent layer. Also the capacitance of the half-plane is reciprocal of the sum of reciprocal capacitance of each layer, and utmost outer layer is calculated consistently as other inner layer.

2.3. Image Strips Technique

Besides SPC technique, there is a different method to resolve the DB problem. Gevorgian [11] proposed "image strips" method. The electric field penetrates through the interface, it forms a virtual parallel capacitor between the IDE and its projected "image strip" on interface as shown in Figure 5. This virtual parallel capacitor contains material with relative permittivity $\epsilon_r - 1$, i.e. the different between the permittivity of the layer and air. Moreover, the effective layer thickness $h_{ef} = h(1 - \frac{\epsilon_{inner}}{\epsilon_{outer}})$ is used to reduce the errors

associated with the imperfect electric wall approximation at the interface. These virtual parallel capacitors of all layers excluding furthest layer, connect in series. The capacitance of furthest layer is calculated as the same as PPC.

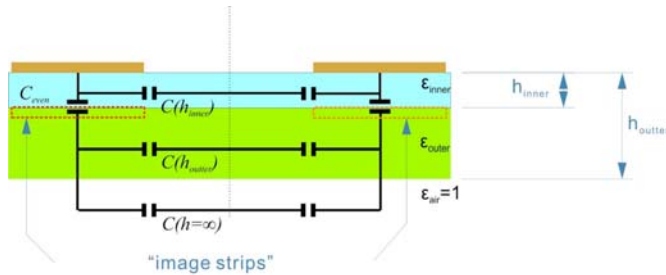


Figure 5: The scheme of "image strips" used in Gevorgian's model.

3. MODELS OF IDCs

With analysis of both IDE and multi-layer structure discussed above, three major models for multi-layer IDCs will be briefly presented here.

3.1. Wu's Model

The first model taking into account a finite layer in multi-layered structure was proposed by Wu *et al.*[12] in 1994. It is typical model combining CM and PPC technique. The model simply considers the "periodical section" formed by two adjacent fingers shown in Figure 6.

The total capacitance of IDCs:

$$C = (N - 1)C_{periodical} \quad (5)$$

where $C_{periodical}$ is the capacitance of periodical section. This capacitance of one half-plane is:

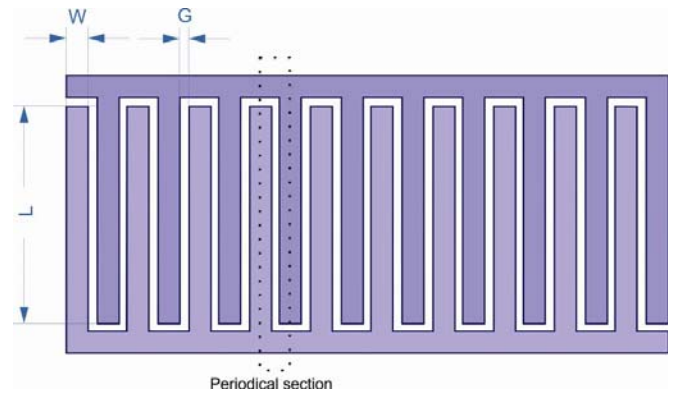


Figure 6: Scheme of different sections used in Wu's model.

$$C_{periodical} = \sum_i^n \epsilon_0 (\epsilon_i - 1) L \frac{K(k_i)}{K(k'_i)} \quad (6)$$

Where k_i and ϵ_i is the CM modulus and permittivity for each substrate respectively with further interface position h .

For another half-plane which is often air layer with infinite height, the capacitance of periodical section becomes:

$$C_{periodical} = \epsilon_0 \epsilon_{air} L \frac{K(k_0)}{K(k'_0)} \quad (7)$$

where k_0 the modulus of CM for air. The CM transformation includes two steps. The first step is to transform the half side of two adjacent fingers in z -plane into t -plane with:

$$t = \sinh\left(\frac{\pi z}{2h_i}\right) \quad (8)$$

And then to transform t -plane to w -plane following the Schwarz-Christoffel transformation. Thus the modulus k_i :

$$k_i = \frac{\sinh\left(\frac{\pi \frac{W}{2}}{2h_i}\right)}{\sinh\left(\frac{\pi \left(\frac{W}{2} + G\right)}{2h_i}\right)} \sqrt{\frac{\sinh^2\left(\frac{\pi \left(\frac{W}{2} + G + W\right)}{2h_i}\right) - \sinh^2\left(\frac{\pi \left(\frac{W}{2} + G\right)}{2h_i}\right)}{\sinh^2\left(\frac{\pi \left(\frac{W}{2} + G + W\right)}{2h_i}\right) - \sinh^2\left(\frac{\pi \frac{W}{2}}{2h_i}\right)}}} \quad (9)$$

For infinite layer, $h \rightarrow \infty$, Eq. (9) becomes:

$$k_0 = \frac{W}{W + 2G} \sqrt{\frac{2W}{2W + G}} \quad (10)$$

3.2. Gevorgian's Model

After Wu's model, Gevorgian *et al.*[5, 6] suggested another model. In his model, the IDE is divided into three parts: "periodical section", "three finger section" and "finger terminals".

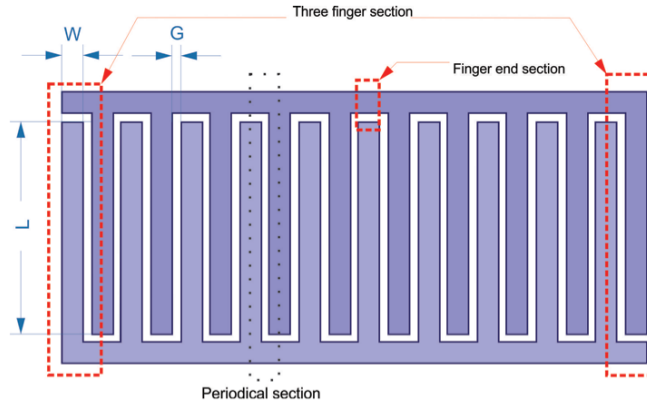


Figure 7: Scheme of different sections used in Gevorgian's model.

Then total capacitance of one half-plane is the summation of all parts:

$$C = (N - 3)C_{periodical} + C_{threefinger} + C_{terminals} \quad (11)$$

These capacitances of one half-plane are:

$$C_{periodical} = \epsilon_0 L \left(\frac{K(k_0)}{K(k'_0)} + (\epsilon_n - 1) \frac{K(k_n)}{K(k'_n)} + \sum_i^{n-1} (\epsilon_i - \epsilon_{i+1}) \frac{K(k_i)}{K(k'_i)} \right) \quad (12)$$

$$C_{threefinger} = 4\epsilon_0 L \left(\frac{K(k_{0,threefinger})}{K(k'_{0,threefinger})} + (\epsilon_n - 1) \frac{K(k_{n,threefinger})}{K(k'_{n,threefinger})} + \sum_i^{n-1} (\epsilon_i - \epsilon_{i+1}) \frac{K(k_{i,threefinger})}{K(k'_{i,threefinger})} \right) \quad (13)$$

$$C_{terminals} = 2NW(2 + \pi)\epsilon_0 L \left(\frac{K(k_{0,terminals})}{K(k'_{0,terminals})} + (\epsilon_n - 1) \frac{K(k_{n,terminals})}{K(k'_{n,terminals})} + \sum_i^{n-1} (\epsilon_i - \epsilon_{i+1}) \frac{K(k_{i,terminals})}{K(k'_{i,terminals})} \right) \quad (14)$$

For another half-plane:

$$C_{periodical} = \epsilon_0 \epsilon_{air} L \frac{K(k_0)}{K(k'_0)} \quad (15)$$

$$C_{threefinger} = 4\epsilon_0 \epsilon_{air} L \frac{K(k_{0,threefinger})}{K(k'_{0,threefinger})} \quad (16)$$

$$C_{terminals} = 2NW(2 + \pi)\epsilon_0 \epsilon_{air} L \frac{K(k_{0,terminals})}{K(k'_{0,terminals})} \quad (17)$$

The CM transformation includes two steps similar to Wu's model, but the function of transforming z-plane into t-plane becomes:

$$t = \cosh^2 \left(\frac{\pi z}{2h_i} \right) \quad (18)$$

And the final formula of modulus k :

$$k_i = \frac{\sinh \left(\frac{\pi W}{2h_i} \right) \sqrt{\cosh^2 \left(\frac{\pi \left(\frac{W}{2} + G \right)}{2h_i} \right) + \sinh^2 \left(\frac{\pi \left(\frac{W}{2} + G \right)}{2h_i} \right)}}{\sinh \left(\frac{\pi \left(\frac{W}{2} + G \right)}{2h_i} \right) \sqrt{\cosh^2 \left(\frac{\pi W}{2h_i} \right) + \sinh^2 \left(\frac{\pi \left(\frac{W}{2} + G \right)}{2h_i} \right)}} \quad (19)$$

$$k_{i,threefinger} = \frac{\sinh \left(\frac{\pi W}{2h_i} \right) \sqrt{1 - \sinh^2 \left(\frac{\pi \left(\frac{W}{2} + G \right)}{2h_i} \right) / \sinh^2 \left(\frac{\pi \left(\frac{W}{2} + W_r + G \right)}{2h_i} \right)}}{\sinh \left(\frac{\pi \left(\frac{W}{2} + G \right)}{2h_i} \right) \sqrt{1 - \sinh^2 \left(\frac{\pi W}{2h_i} \right) / \sinh^2 \left(\frac{\pi \left(\frac{W}{2} + W_r + G \right)}{2h_i} \right)}} \quad (20)$$

$$k_{i,terminals} = \frac{\sinh \left(\frac{\pi W}{2h_i} \right) \sqrt{1 - \sinh^2 \left(\frac{\pi \left(\frac{W}{2} + G \right)}{2h_i} \right) / \sinh^2 \left(\frac{\pi \left(\frac{3W}{2} + G \right)}{2h_i} \right)}}{\sinh \left(\frac{\pi \left(\frac{W}{2} + G \right)}{2h_i} \right) \sqrt{1 - \sinh^2 \left(\frac{\pi W}{2h_i} \right) / \sinh^2 \left(\frac{\pi \left(\frac{3W}{2} + G \right)}{2h_i} \right)}} \quad (21)$$

For infinite layer, $h \rightarrow \infty$, Eq. (19)-(21) become simple equations:

$$k_0 = \frac{W}{W + 2G} \quad (22)$$

$$k_{0,threefinger} = \frac{W}{W+2G} \sqrt{\frac{1 - \left(\frac{W+2G}{W+2W_T+2G}\right)^2}{1 - \left(\frac{W}{W+2W_T+2G}\right)^2}} \quad (23)$$

$$k_{0,terminals} = \frac{W}{W+2G} \sqrt{\frac{1 - \left(\frac{W+2G}{3W+2G}\right)^2}{1 - \left(\frac{W}{3W+2G}\right)^2}} \quad (24)$$

3.3. Igreja's Model

Igreja and Dias[7, 8] selected "interior" (periodical) and "external" sections shown in Figure 8 for investigation. According to permittivity of substrates, PPC or SPC technique is combined with CM technique.

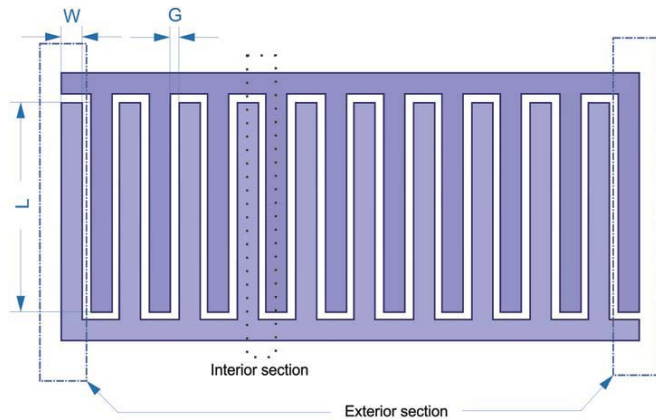


Figure 8: Scheme of different sections used in Igreja's model[7, 8].

The total capacitance of one half-plane:

$$C = (N-3)C_I + 2\left(\frac{C_I C_E}{C_I + C_E}\right) \quad (25)$$

where C_I and C_E are the capacitances of interior and external sections. These capacitances in the PPC situation, the permittivity monotonic decreases, are:

$$C_{I,PPC} = \epsilon_0 L \left(\epsilon_n \frac{K(k_{n,I,PPC})}{K(k'_{n,I,PPC})} + \sum_i^{n-1} (\epsilon_i - \epsilon_{i+1}) \frac{K(k_{i,I,PPC})}{K(k'_{i,I,PPC})} \right) \quad (26)$$

$$C_{E,PPC} = \epsilon_0 L \left(\epsilon_n \frac{K(k_{n,E,PPC})}{K(k'_{n,E,PPC})} + \sum_i^{n-1} (\epsilon_i - \epsilon_{i+1}) \frac{K(k_{i,E,PPC})}{K(k'_{i,E,PPC})} \right) \quad (27)$$

In the SPC situation, these capacitances are:

$$\frac{1}{C_{I,SPC}} = \frac{1}{\epsilon_0 L} \left(\frac{1}{\epsilon_n} \frac{K(k'_{i,I,SPC})}{K(k_{i,I,SPC})} + \sum_i^{n-1} \left(\frac{1}{\epsilon_i} - \frac{1}{\epsilon_{i+1}} \right) \frac{K(k'_{i,I,SPC})}{K(k_{i,I,SPC})} \right) \quad (28)$$

$$\frac{1}{C_{E,SPC}} = \frac{1}{\epsilon_0 L} \left(\frac{1}{\epsilon_n} \frac{K(k'_{i,E,SPC})}{K(k_{i,E,SPC})} + \sum_i^{n-1} \left(\frac{1}{\epsilon_i} - \frac{1}{\epsilon_{i+1}} \right) \frac{K(k'_{i,E,SPC})}{K(k_{i,E,SPC})} \right) \quad (29)$$

For another half plane, these capacitances are simplified as:

$$C_I = \epsilon_0 \epsilon_{air} L \frac{K(k_{0,I})}{K(k'_{0,I})} \quad (30)$$

$$C_E = \epsilon_0 \epsilon_{air} L \frac{K(k_{0,E})}{K(k'_{0,E})} \quad (31)$$

To get the CM modulus for PPC case, Igreja and Dias[7, 8] transform the selected region in four steps. When placing the half side of two adjacent fingers in x-plane, the points inside this half side are transformed into z-plane with function:

$$z = \frac{4K(c)}{2(W+G)} x \quad (32)$$

where

$$c = \frac{\left(v_2 \left(0, e^{-4\pi \frac{h_i}{2(W+G)}} \right) \right)^2}{\left(v_3 \left(0, e^{-4\pi \frac{h_i}{2(W+G)}} \right) \right)} \quad (33)$$

And transforming z-plane into t-plane with:

$$t = sn(z, c) \quad (34)$$

Before using Schwarz-Christoffel transformation, the t-plane is transformed into y-plane with:

$$y = \frac{t}{t_2} \sqrt{\frac{t_4^2 - t_2^2}{t_4^2 - t^2}} \tag{35}$$

where

$$t_2 = \operatorname{sn}\left(K(c) \frac{W}{W+G}, c\right) \tag{36}$$

$$t_4 = \frac{1}{c} \tag{37}$$

Then after Schwarz-Christoffel transformation,

$$k_{i,l,PPC} = t_2 \sqrt{\frac{t_4^2 - 1}{t_4^2 - t_2^2}} \tag{38}$$

In Eq. (33)-(38), $\operatorname{sn}(a, b)$ is the Jacobi elliptic function of modulus b ; v_2 and v_3 are the Jacobi 2nd and 3rd theta functions. For infinite layer, $h \rightarrow \infty$, Eq. (38) becomes:

$$k_0 = \sin\left(\frac{\pi}{2} \frac{W}{W+G}\right) \tag{39}$$

Later, Igreja and Dias[8] extended the model using SPC with replacing Eq. (38) with:

$$k_{i,l,SPC} = t_2 \tag{40}$$

The calculation of t_2 is the same as PPC. And the CM modulus of external section becomes:

$$k_{i,e,SPC} = \frac{1}{t_3} \sqrt{\frac{t_5^2 - t_3^2}{t_5^2 - 1}} \tag{41}$$

where,

$$t_3 = \cosh\left(\frac{\pi G}{8 \frac{h_i}{W}}\right) \tag{42}$$

$$t_5 = \cosh\left(\frac{\pi(2W+G)}{8 \frac{h_i}{W}}\right) \tag{43}$$

4. COMPARISON AND APPLICATIONS OF MODELS

The models in the previous section synthesize the analysis of both IDE and multi-layered structures. The distinct difference among these models is the selection of region except the periodical section. There is only periodical section in Wu’s model, but there are external sections in the other two. Gevorgian’s model treats two external sections into “three-finger” sections and directly sums its capacitance into total capacitance. On the contrary, Igreja’s model leaves two external sections individual and connects them to the periodical section in parallel.

Furthermore, modeling of the periodical section has various processes. Wu’s and Gevorgian’s models use two-step transformation, but with different transformation functions before applying CM technique. Therefore the final expressions are dissimilar. And Igreja’s model uses four-step transformation, making the geometrical parameters dimensional.

Besides models themselves, the intention of developing models is different. In past years, IDCs are frequently used in lumped elements for microwave integrated circuits. With ferroelectric thin-film, IDCs can also be used a voltage-controlled tunable device. [12] At that ages, although the integrated circuit design including IDCs may be performed by computer software, it is time-consuming. Thus Wu’s and Gevorgian’s models aim to be tools for computer-aided design for microwave integrated circuits. Later, Gevorgian’s model becomes a useful tool for extraction of the dielectric properties of the ferroelectric layers using the measured impedances of tunable microwave devices.[13-15] In contrast, Igreja’s model aims to the extraction of information as a chemo-capacitor sensor with IDEs. [9, 16]

5. CONCLUSIONS AND PERSPECTIVES

In this article, we have summarized the techniques used in modeling the closed form expression for multi-layered IDCs. The interface between different substrates is an important factor in multi-layered structure, which determines the boundary condition in electric field distribution and altering conformal mapping process. The techniques for resolving multi-layered structure are varied due to different boundary conditions. For general case of monotonic decreasing permittivity, we use the parallel partial capacitance technique to consider each layer separately. However, in the case of monotonic increase, there are different

choices. We are able to use series partial capacitance technique suggested by Ghione and Igreja, or image strip technique suggested by Gevorgian.

For considering single layer, the conformal mapping, especially Schwarz-Christoffel transformation, is used to analogize different sections to a parallel plate capacitor. Wu, Gevorgian and Igreja suggested different conformal mapping processes and gave the final form of closed form expression. Moreover, the properties of IDE can be also added to the model with modified the effective width of electrodes.

Although these models are widely used in different aspects, there are some limitations when applying the closed form analytic expressions for IDCs. Particularly, for IDCs with tunable ferroelectric film, in an extreme case, the permittivity does not increase nor decrease, causing the issue of applying current models. In a mixed case, the PC method does not provide, in general, a satisfactory approximation.

In terms of future research and application for the characterization of tunable ferroelectric films, although the CM techniques transform IDCs into equivalent parallel capacitors by considering the electrical potential, the electric field distribution caused by IDEs in the ferroelectric film is non-uniform. Therefore, the induced changes of ferroelectric thin-film in the permittivity are also non-uniform. It causes that the in-plane properties of ferroelectric are not well studied by using these models. It is necessary to build modified models to ferroelectric films based IDCs.

REFERENCE

- [1] Hoffmann RK, Howe HH. Handbook of microwave integrated circuits. Norwood, MA: Artech House; 1987.
- [2] Rautio JC. An investigation of microstrip conductor loss. Microwave Magazine, IEEE. 2000;1(4):60-7.
- [3] Kochanov ES. Parasitic capacitances in printed wiring radio equipment. Telecommunications and Radio Engineering. 1987;22:129-32.
- [4] Veyres C, Fouad Hanna V. Extension of the application of conformal mapping techniques to coplanar lines with finite dimensions. International Journal of Electronics. 1980;48(1):47-56.
- [5] Gevorgian S, Carlsson E, Rudner S, Wernlund LD, Wang X, Helmersson U. Modelling of thin-film HTS/ferroelectric interdigital capacitors. Microwaves, Antennas and Propagation, IEE Proceedings. 1996;143(5):397-401.
- [6] Gevorgian SC, Martinsson T, Linner PLJ, Kollberg EL. CAD models for multilayered substrate interdigital capacitors. IEEE Transactions on Microwave Theory and Techniques. 1996;44(6):896.
- [7] Igreja R, Dias CJ. Extension to the analytical model of the interdigital electrodes capacitance for a multi-layered structure. Sensors & Actuators: A Physical. 2011;172(2):392-9.
- [8] Igreja R, Dias CJ. Analytical evaluation of the interdigital electrodes capacitance for a multi-layered structure. Sensors & Actuators: A Physical. 2004;112(2):291-301.
- [9] Kitsara M, Goustouridis D, Chatzandroulis S, Chatzichristidi M, Raptis I, Ganetsos T, *et al.* Single chip interdigitated electrode capacitive chemical sensor arrays. Sensors and Actuators B: Chemical. 2007;127(1):186-92.
- [10] Ghione G, Goano M. Revisiting the partial-capacitance approach to the analysis of coplanar transmission lines on multilayered substrates. Microwave Theory and Techniques, IEEE Transactions on. 2003;51(9):2007-14.
- [11] Gevorgian S. Modeling. Ferroelectrics in Microwave Devices, Circuits and Systems. Engineering Materials and Processes: Springer London; 2009. p. 245-86.
- [12] Wu HD, Zhang ZH, Barnes F, Jackson CM, Kain A, Cuchiaro JD. Voltage tunable capacitors using high temperature superconductors and ferroelectrics. IEEE Transactions on Applied Superconductivity. 1994;4(3):156-60.
- [13] Yang ZB, Hao JH. In-plane dielectric properties of epitaxial $\text{Ba}_{0.7}\text{Sr}_{0.3}\text{TiO}_3$ thin films grown on GaAs for tunable device application. Journal of Applied Physics. 2012;112(5):054110.
- [14] Simon WK, Akdogan EK, Safari A, Bellotti JA. In-plane microwave dielectric properties of paraelectric barium strontium titanate thin films with anisotropic epitaxy. Applied Physics Letters. 2005;87(8):082906.
- [15] Zhang XY, Wang P, Sheng S, Xu F, Ong CK. Ferroelectric $\text{Ba}_x\text{Sr}_{1-x}\text{TiO}_3$ thin-film varactors with parallel plate and interdigital electrodes for microwave applications. Journal of Applied Physics. 2008;104(12):124110.
- [16] Igreja R, Dias CJ. Dielectric response of interdigital chemocapacitors: The role of the sensitive layer thickness. Sensors and Actuators B: Chemical. 2006;115(1):69-78.

Received on 10-05-2014

Accepted on 10-06-2014

Published on 28-08-2014

<http://dx.doi.org/10.15379/2408-977X.2014.01.01.1>

© 2014 Mak and Hao ; Licensee Cosmos Scholars Publishing House.

This is an open access article licensed under the terms of the Creative Commons Attribution Non-Commercial License (<http://creativecommons.org/licenses/by-nc/3.0/>), which permits unrestricted, non-commercial use, distribution and reproduction in any medium, provided the work is properly cited.